Thermoelastic Pressure Waves Induced Inside the Human Head by RF Pulses From High Pass Birdcage Coils

Z. Wang[1], J. C. Lin[2]

[1]Center for NMR Research, Penn State College of Medicine, Hershey, PA, United States, [2]Electrical & Computer Engineering, Bioengineering, University of Illinois-Chicago, Chicago, IL, United States

Introduction

A number of researchers have studied the microwave auditory effect over the years (1-3). With the development of high-field strength and ultra-fast MRI instruments, there have been increasing concerns about its safety and potential health hazards. Microwave auditory effect has been widely reported as a biological response evoked by irradiating the human head with pulsed microwave energy. The transduction mechanism for the auditory effect is understood to be a microwave pulse induced thermoelastic expansion in brain tissue, due to the small but rapid temperature rise in soft tissues, which generates an acoustic wave of pressure. Experimental and theoretical studies have shown that microwave-induced auditory sensation in human and animal does not arise from an interaction of microwave pulses directly with the auditory nerves or neurons along the auditory neural pathways of the central nervous system. The microwave pulse, upon absorption by soft tissues in the head, launches a thermoelastic wave of acoustic pressure, which travels by bone conduction to the inner ear.

Here we present numerical computations for the thermoelastic wave pressure in a human head in high-pass birdcage coils for MRI. The frequencies are 64 MHz, 300 MHz, and 400 MHz, or magnetic flux densities of 1.5 T, 7.0 T, and 9.4T, respectively. We used 100-μs and 200-μs pulses. The human head model without shoulder and neck, with 3-mm resolution, was used in the calculation. The pressures and corresponding power spectra at the center of the head are also given. The results showed that RF-induced thermoelastic pressure wave in the head depend on pulse width and SAR or absorbed power. Due to the irregular shape and heterogeneity of tissues in the head, the pressure wave distribution is complex.

Method

In this study we employed a high-pass birdcage MRI coil (15-cm radius; 16-cm length) with 16 rungs. Each rung was 1-cm wide (copper). The radius and length of the shield were 19 cm and 24 cm, respectively. Ideal current sources were placed at the midpoint of each end-ring element of the MRI coil; a 22.5-degree phase-shift was set between elements. The human head model without the shoulder and neck was adopted. The resolution for the head model is 3x3x3 mm. A Four-Cole-Cole extrapolation was used to determine values for the dielectric properties of the tissues at 64 MHz, 300MHz and 400 MHz. Tissue parameters used in the computer simulation are available from the Brooks Air Force Laboratory database. The two Lame's constants used are: for soft tissue, λ=2.24 GPa, μ=1.052x10^{-6} Gpa, and for bone and tooth tissue, λ=6.923 GPa, μ=4.615 Gpa. The coefficients of linear thermal expansion are α =4.1x10^{-5} 1/^{o}C and α=1.06x10^{-5} 1/^{o}C, respectively, for the soft and hard tissues. We also use the error function as the modulation functions for 100-μs and 200-μs pulse to reduce higher frequency components that cannot be efficiently computed by the FDTD method.

Result and Discussion

We normalized the input current source amplitude to 100 mA. The SAR results are shown in Fig 1. Generally, the SAR was frequency dependent, as expected, and it increased as the frequency increased. At the lower frequency (64 MHz), the maximum SAR was located in the peripheral. The SAR values decreased somewhat, in deeper tissues of the head. Note that the SAR reached zero in the center of the head. With increasing frequencies, the higher SAR moved to inside the head, thus the SAR in the central part of the head was considerably higher in comparison. The bright spots are obvious at 300 MHz and 400 MHz. The human head model is asymmetric and heterogeneous. Although more uniform currents were obtained in the rungs due to the use of ideal current distributions, the RF field inside the coil was less circularly polarized than for a homogeneous, symmetric sphere. The B_1 field homogeneity was degraded, and had led to higher SAR.

Only the computed distribution of pressure waves at 300 MHz is shown in Fig 2. The sequences and waveforms of induced pressures were much more complex than those of the sphere model. The differences are related to the complex shape and heterogeneity of the head model. The graphs showed that the pressure wave was initiated in the location where a large SAR appeared and was negative initially. The pressure wave then propagated toward the center of the head. When it reached the center, the pressure became positive and the wave started to propagate outward to the boundary. When it reached the boundary, the pressure became negative again and then reverberated several times. The pressure sequences shown in these figures began at 20 μs, and ended at 240 μs in time step of 20 μs. At different frequencies, the pressure distributions are totally different because the different SAR distributions inside the head. Due to the normalization of amplitude of current source at 100 mA, the SAR and pressure distribution inside the human head at 400 MHz was higher than the result at 300 MHz and 64 MHz. For the 200-μs pulse, at 64 MHz, the peak pressure was 0.0169 mPa. At 300 MHz, the peak pressure was 1.18 mPa and higher than that at 64 MHz. The peak pressures at 400 MHz had the highest value, which was 3.57 mPa. On the other hand, for the 100-μs pulse, the peak pressure was 0.0243 mPa at 64 MHz, 1.19 mPa at 300 MHz, and 3.31 mPa at 400 MHz. These values are different due to the absorption power and pulse width. Therefore, pressure distributions are depended on the frequencies, absorption power and pulse width.

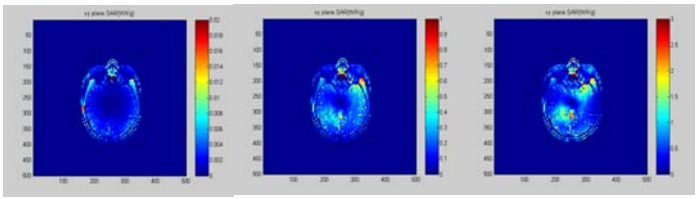

Fig 1 SAR Distribution

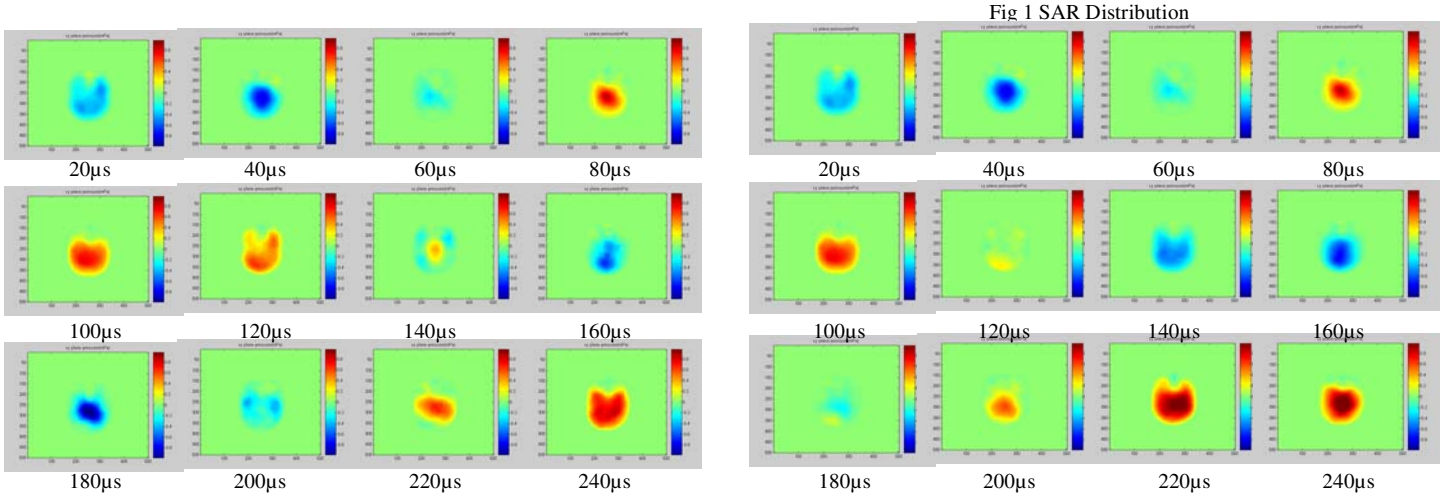

Fig 2 Pressure Distributions at 300 MHz

Reference

1. J. C. Lin, IEEE MTT 25:P605 (1977)
2. J. C. Lin, Proc. IEEE 68:P67 (1980)
3. Y. Watanabe et al, IEEE MTT 48:P2126 (2000)